JOURNAL OF MATERIALS SCIENCE 32 (1997) 3659–3665

Preparation and properties of barium titanate glass-ceramics sintered from sol–gel-derived powders

KUI YAO*, LIANGYING ZHANG, XI YAO
Electronic Materials Research Laboratory, Xi'an Jiaotong University, Xi'an 710049, People's Republic of China

WEIGUANG ZHU
Microelectronic Center, School of Electrical and Electronic Engineering, Nanyang Technological University, Singapore 639798

Homogeneous Ba–Ti–B–Si, Ba–Ti–Al–Si and Ba–Ti–B gels have been successfully prepared by the sol–gel process. A novel method is presented for fabricating barium titanate glass-ceramics by sintering the gel powders with small barium titanate crystallites. The structural development, grain size, crystallization process and dielectric properties were systematically studied by differential thermal analysis, thermogravimetric analysis, X-ray diffraction techniques, scanning electron microscopy and dielectric measurements. The glass-ceramic samples were sintered at lower temperatures compared to the barium titanate ceramic sintering, and showed improved dielectric properties. It was found that the small size effect of the barium titanate grains on the dielectric constant in the glass-ceramics was quite evident. Ferroelectric hysteresis loop analyses were also performed to manifest the ferroelectric nature of the barium titanate grains *in situ* grown from the gels.

1. Introduction

Ferroelectric ceramics have been widely used for multilayer and thick-film capacitors, and in the applications of electronic components [1–6]. With the advance of modern technology and miniaturization of electronic devices, reduction of thickness for each capacitor layer and great homogeneity are highly required. The improvement of a homogeneous mixture of all the constituents in the dielectric medium becomes very essential.

Glass phase is one of the important constituents of electronic pastes for multilayer and thick-film applications. The appropriate addition of a glass ingredient is useful to reduce the sintering temperature to make the sintering process more compatible with cheap metal electrodes, and even to improve the properties. In the case of thick-film technology, glass is especially necessary as the binding phase. In the conventional production process of ferroelectric multilayer and thick-film capacitors, the pastes are prepared by mixing powders of ferroelectric phase and glass phase using the ball-mill process [3, 4, 7]. The agglomeration of fine ferroelectric powders limits the improvement of the homogeneity of the mixture [8, 9]. As the thickness of monolayers of the capacitors decreased, inhomogeneity may result in a deterioration of properties and a reduction in reliability. It is noted that the ferroelectric glass-ceramics have fine structures, in which ferroelectric grains of hundreds and even tens of nanometres are dispersed homogeneously in glass phases [10–13]. Thick-film capacitors using melting–quenching derived glass-ceramics as the medium have been fabricated [14, 15].

The melting–quenching technique requires elevated temperature to melt all components. It has obvious disadvantages in preparing ferroelectric glass-ceramics in which some components have high melting temperatures and/or high volatility. Therefore, the composition of the thus prepared glass-ceramic is limited. It is also difficult to prepare glass-ceramic thick-film medium with a very high dielectric constant. The reason is that a higher melting temperature and more rapid quenching are required as the ferroelectric constituent increases. During the process of preparing barium titanate ($BaTiO_3$) glass-ceramic thick-film capacitors with high permittivity, $BaTiO_3$ ceramic powders have to be added and mixed with the glass powders by the ball-mill method. This is because the $BaTiO_3$ crystals precipitated from the melting–quenching derived glass are insufficient [15]. Thus, part of the merit of this method is lost apparently by virtue of introducing such a mechanical mixing process.

**Present address:* School of Electrical and Electronic Engineering, Nanyang Technological University, Nanyang Avenue, Singapore 639798.

0022–2461

Recently, we reported work on fine-grained barium titanate glass-ceramics prepared by annealing the gel bulks derived from the sol–gel method without going through the melting and quenching procedure [16]. This technique provides a new approach to mixing ferroelectric phase and glass phase homogeneously. In this paper, we report our experimental results and study on the structural features and dielectric properties of the $BaTiO_3$ based glass-ceramics prepared by sintering sol–gel-derived gel powders.

2. Experimental procedure

Three $BaTiO_3$-based glass-ceramic samples with high barium and titanium content were prepared by the sol–gel method. The composition ratios of these samples were Ba : Ti : B (BTB) = 1.12 : 1 : 0.28; Ba : Ti : B : Si (BTBS) = 5.5 : 5 : 1 : 1; Ba : Ti : Al : Si (BTAS) = 5.5 : 5 : 1 : 1. The sol–gel-derived $BaTiO_3$ ceramic samples with the composition ratio of Ba : Ti (BT) = 1 : 1 were also prepared for comparison. The precursors used were barium acetate ($Ba(CH_3COO)_2$), titanium butoxide ($Ti(OCH_2CH_2CH_2CH_3)_4$), ethyl silicate ($Si(OCH_2CH_3)_4$), aluminium isopropoxide ($Al(OCH(CH_3)_2)_3$) and tripropyl borate ($B(OCH_2CH_2CH_3)_3$). These precursors were mixed according to sample compositions. The detailed preparation procedure was described elsewhere [16]. After tens of hours, all the solutions turned into transparent, homogeneous gels.

After ageing and drying, the BTB and BTBS gels were pyrolysed at 850 °C, whereas BT and BTAS gels were pyrolysed at 900 °C. Small $BaTiO_3$ crystallites were formed in these firing processes. The fired gels were then crushed and ground by ball milling with ethanol for 1 h to obtain fine powders. Following that, the powders were pressed into disc-shaped pellets with a diameter of 10 mm. The pellets were subsequently sintered in air at various temperatures for 1 h. The surfaces of these glass-ceramic and ceramic samples were polished before the Pd–Ag paste electrodes were formed at 700 °C.

After etching in 5% hydrofluoric acid and cleaning in acetone, the cross-sections of the samples were examined using a Cambridge Stereoscan 360 scanning electron microscope (SEM). The crystal structures were examined by a D/max-2400 X-ray diffractometer (XRD). A differential thermal analyser (DTA) of Du Pond DTA1600 and a Du Pond TG2000 thermogravimetric analyser (TGA) were used to study the thermal behaviour of the gels. The particle sizes of gel-derived powders were measured using a particle size analyser of Model BI-90. The dielectric properties of the ceramic and glass-ceramic pellets were characterized using HP4274A and HP4275A impedance analysers. The ferroelectric hysterisis loops of the glass-ceramic samples were measured using a modified Sawyer–Tower bridge.

3. Results and discussion

The thermal analysis results of the BTB gel with a heating rate of 10 °C min^{-1} are shown in Fig. 1. In the TGA curve, weight loss at a temperature below 500 °C is attributed to the evaporation of the solvent and the decomposition of organic radicals. The another notable weight loss takes place at a temperature of about 680 °C. Similar phenomena have been observed in BT, BTBS and BTAS samples. It was noted in our experiments that all the samples were light grey after annealing at 600 °C but turned white after annealing above 700 °C. It was also noted in these samples that some minor phases, like $BaCO_3$, decomposed in this temperature range. So the weight loss at around 680 °C is believed to be due to the burning of the residual carbon and the decomposition of a small amount of the $BaCO_3$ phase.

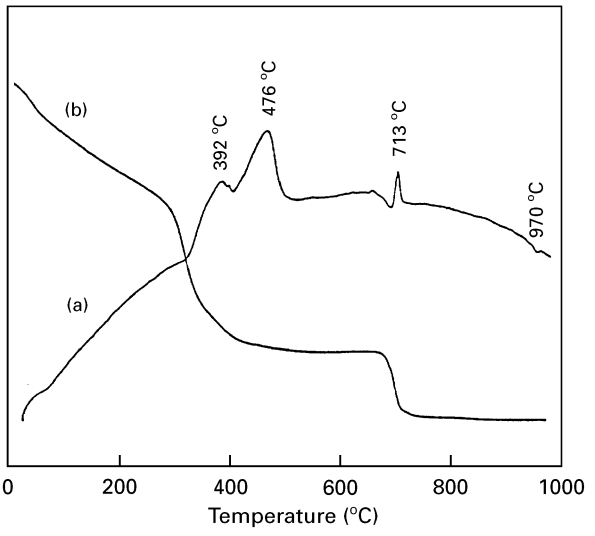

Figure 1 (a) Differential thermal analysis and (b) thermogravimetric analysis curves of the BTB gel with a heating rate of 10 °C min^{-1} in O_2.

There is a total of four exothermic peaks at 392, 476, 713 and 970 °C in the DTA curve of the BTB gel, as seen in Fig. 1. The first two peaks are attributed to the thermal decomposition of the organic radicals. Each of the other two exothermic peaks follows an endothermic peak. The endothermic peak indicates a softening process in the glass phase. The exothermic peak at 713 °C is believed to be due to the crystallization of $BaTiO_3$ phase and the peak at 970 °C for the formation of BaB_2O_4 phase.

The X-ray diffraction patterns for the BTB samples annealed in air for 1 h at different temperatures are shown in Fig. 2. These X-ray results show that the $BaTiO_3$ phase starts to crystallize at 600 °C, and a large amount of the $BaTiO_3$ phases is formed at 800 °C. A minor trace of $BaCO_3$ phase is detected at 600 °C and is decomposed at 800 °C. A secondary phase, BaB_2O_4 phase, is formed at 1000 °C, as shown in Fig. 2c. For the BT gel, similar results of the presence of a small amount of $BaCO_3$ phase and the weight loss at about 680 °C in the TGA curves have also been reported in the literature [17–20].

The thermal analysis results for the BTBS gels are shown in Fig. 3. An almost identical TGA behaviour is observed. For the DTA curve of this sample, the two exothermic peaks at 384 and 437 °C are attributed to the thermal decomposition of organic components.

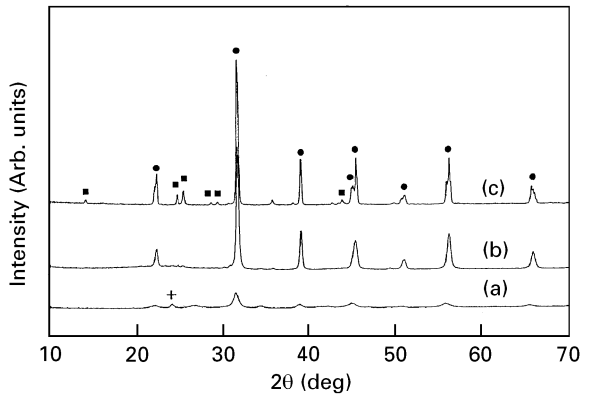

Figure 2 X-ray diffraction patterns of BTB samples annealed at different temperatures in air for 1 h: (a) 600 °C, (b) 800 °C and (c) 1000 °C; (●) $BaTiO_3$, (+) $BaCO_3$, (■) BaB_2O_4.

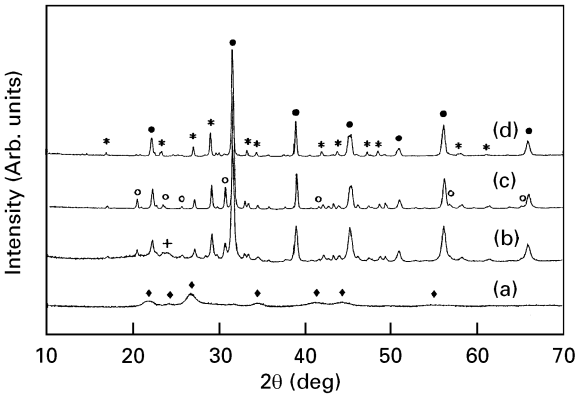

Figure 4 X-ray diffraction patterns of BTBS samples annealed at different temperatures in air for 1 h: (a) 600 °C, (b) 800 °C, (c) 900 °C, (d) 1000 °C; (●) $BaTiO_3$, (◆) unidentified phase, (+) $BaCO_3$, (○) $Ba_2Ti_2B_2O_9$, (*) $Ba_2TiSi_2O_8$.

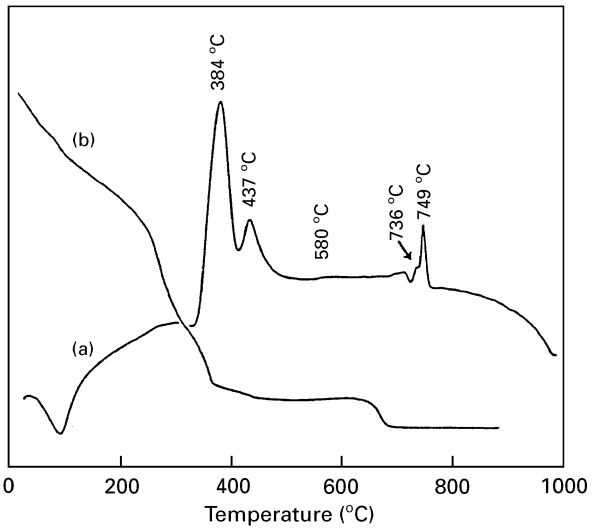

Figure 3 (a) Differential thermal analysis and (b) thermogravimetric analysis curves of the BTBS gel with a heating rate of 10 °C min^{-1} in O_2.

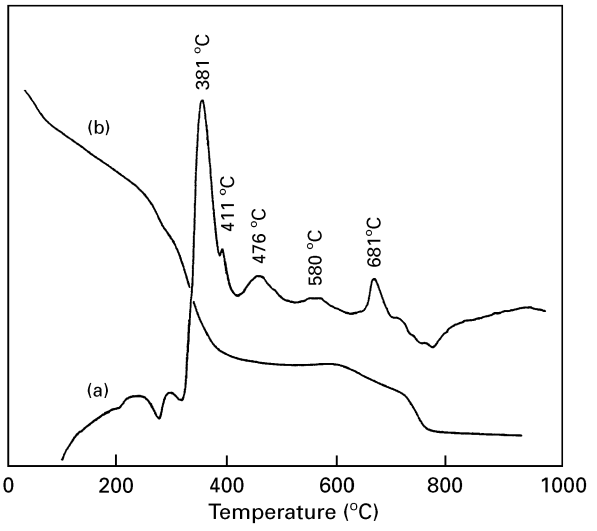

Figure 5 (a) Differential thermal analysis and (b) thermogravimetric analysis curves of the BTAS gel with a heating rate of 10 °C min^{-1} in O_2.

A weak peak around 580 °C is believed to be due to the crystallization of an unidentified minor phase. The endothermic peak at around 720 °C indicates that the glass phase softens at this temperature, followed by some strong exothermic peaks due to the crystallization process. The peaks at around 736 °C are believed to be due to the crystallization of $Ba_2TiSi_2O_8$ and $Ba_2Ti_2B_2O_9$ phases, and the last peak at 749 °C to be due to the crystallization of $BaTiO_3$ phase.

The X-ray diffraction patterns for these BTBS samples are presented in Fig. 4. It is clear that an unidentified phase, which is not observed in the BT gel, forms in this gel when annealed at 600 °C. This unidentified phase is unstable and hence disappears at 800 °C, while the $BaTiO_3$, $Ba_2TiSi_2O_8$ and $Ba_2Ti_2B_2O_9$ phases are formed in this temperature range. Minor $BaCO_3$ phase is also observed, which decomposed at higher temperature. As the temperature increased to 1000 °C, the $Ba_2Ti_2B_2O_9$ phase also decomposed, leaving only the $BaTiO_3$ phase and some of the $Ba_2TiSi_2O_8$ phase.

The thermal analysis results of BTAS gel are given in Fig. 5. The weight loss between 600 and 750 °C can be attributed to the burning off the remnant carbon and the decomposition of a small amount of the $BaCO_3$ phase. In the DTA curve, the exothermic peaks at 381, 411 and 476 °C are attributed to the thermal decomposition of organic components, while the peak at 580 °C is believed to be due to the crystallization of the same unidentified phase as in the BTBS system. The last peak at 681 °C is due to the formation of the $BaTiO_3$ phase.

The X-ray diffraction patterns for the BTAS samples in Fig. 6 show that the unidentified phase is formed at 600 °C and disappears at 800 °C. $BaTiO_3$ phase, and minor amounts of $Ba_2TiSi_2O_8$ and $BaCO_3$ phases are also formed when annealed above 700 °C. Both the $BaCO_3$ and $Ba_2TiSi_2O_8$ phases are decomposed at higher temperatures, and a little secondary $BaAl_2Si_2O_8$ phase appears after annealing above 1100 °C, as shown in Figs. 6d and e.

Table I gives the volume average particle size and the volume median diameters of the powders after ball milling. It is seen that they are in the range of several hundreds of nanometres, and that the particle sizes for the BTB, BTBS and BTAS glass-ceramic powders are

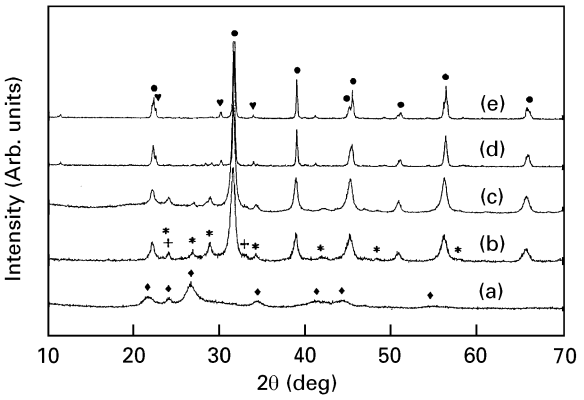

Figure 6 X-ray diffraction patterns of BTAS samples annealed at different temperatures in air for 1 h: (a) 600 °C, (b) 700 °C, (c) 800 °C, (d) 1100 °C and (e) 1250 °C; (●) $BaTiO_3$, (◆) unidentified phase, (+) $BaCO_3$, (∗) $Ba_2TiSi_2O_8$, (♥) $BaAl_2Si_2O_8$.

TABLE I Particle sizes of the gel-derived powders after ball milling with ethanol for 1 h

Samples	Volume average size (nm)	Volume median diameter (nm)
BT	683	589
BTB	314	284
BTBS	309	276
BTAS	495	372

slightly smaller than that of the BT ceramic powders. It is well known that powders are usually aggregations of many small grains [8, 19–21]. In fact, the grain sizes of the sol–gel-derived $BaTiO_3$ are only tens of nanometres to one hundred nanometres when the annealing temperature is below 900 °C [20, 21]. It has been shown by some researchers that the tetragonality of the $BaTiO_3$ crystal depends on the crystallite size and the transformation from tetragonal to cubic symmetry occurs at a critical size of about 120 nm at room temperature [22]. This fact explains why the $BaTiO_3$ crystal structure is the cubic phase when annealed at low temperatures, as shown in our X-ray diffraction patterns of BTB, BTBS and BTAS samples.

Fig. 7 gives the cross-sectional micrographic pictures of the BT, BTB, BTBS and BTAS samples sintered at different temperatures. Well-sintered $BaTiO_3$ ceramic samples can only be obtained when annealed at very high temperatures of 1300 °C. The average grain size after annealing at 1300 °C for 1 h is above 10 μm. The grain boundaries and the ferroelectric domains can be clearly seen in Fig. 7a. The BTB sample can be well sintered at a temperature of 1000 °C and the average grain size is about 1–2 μm. The grain boundaries are not distinct. The BTBS sample is sintered at 1000 °C and the average grain size after 1 h annealing is about several hundred nanometres. The BTAS samples can be well sintered at 1200 °C and the average grain size is also about hundreds of nanometres. No ferroelectric domains for the small $BaTiO_3$ grains grown in the glass-ceramic samples can be seen from the scanning electron micrographs.

Some pores are observed in the scanning electron micrograph of the BTBS sample in Fig. 7c. Most of

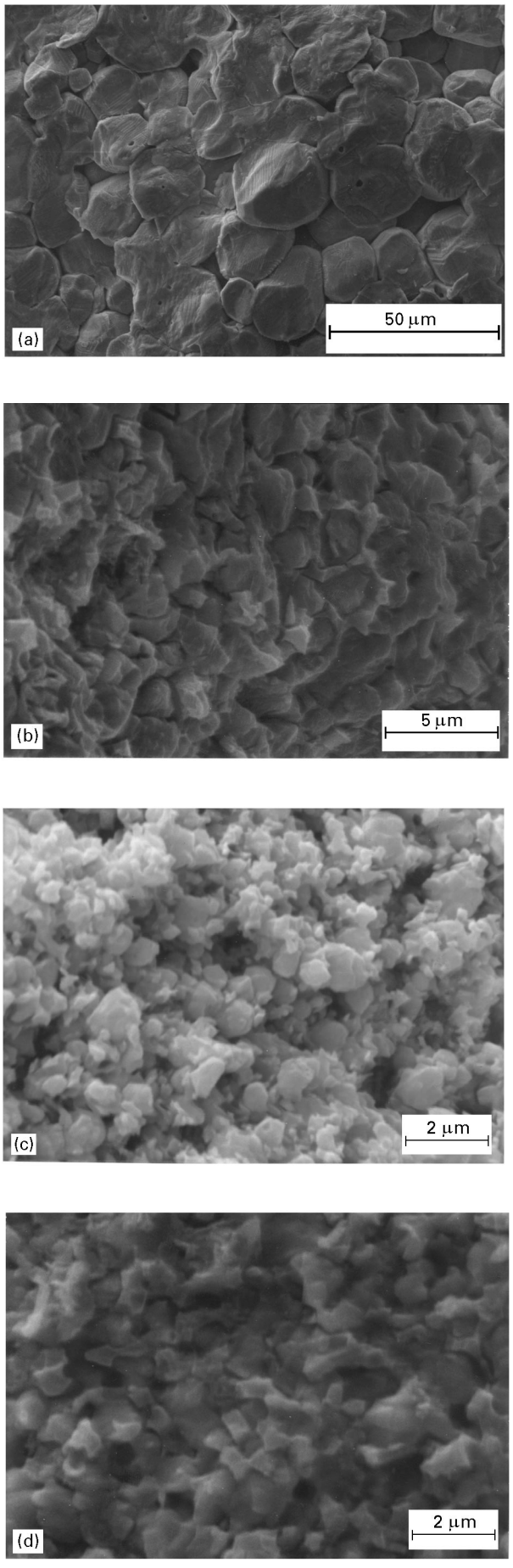

Figure 7 Scanning electron micrographs of the cross-sections of the BT ceramic and glass-ceramic samples sintered at various temperatures in air for 1 h. The samples are etched by the hydrofluoric acid: (a) BT, 1300 °C, (b) BTB, 1000 °C, (c) BTBS, 1000 °C and (d) BTAS, 1200 °C.

these pores are caused by the etching process and the subsequent ultrasonic cleaning process. The cross-sectional micrographic picture of the freely etched sample after annealing at 1000 °C for 1 h is shown in Fig. 8. This picture shows that the original sample is well sintered at this temperature and has a dense structure.

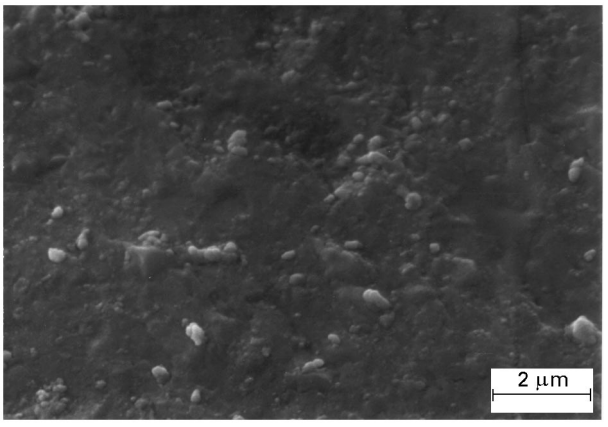

Figure 8 Scanning electron micrograph of the fresh cross-section of the BTBS sample sintered at 1000 °C in air for 1 h.

Because the glass phases and the $BaTiO_3$ phase are homogeneously mixed, the glass-ceramic samples can be sintered well at much lower temperature than the pure $BaTiO_3$ ceramic. Much smaller sized $BaTiO_3$ grains are obtained in the sintered glass-ceramic systems than in the glass-free ceramic system.

The temperature dependence of the dielectric constant for the BT ceramic and glass-ceramic samples annealed at different temperatures for 1 h in air is shown in Fig. 9. For the BT ceramic and the three glass-ceramic samples, the dielectric constants are small when the annealing temperature is far below the sintering temperature. One reason for the small dielectric constant is the high porosity of the samples when the annealing temperature is too low. Another reason may be that the $BaTiO_3$ crystallites are so small that ferroelectricity is very weak. With increasing annealing temperature, the dielectric constants of all the samples are increased notably. The difference between the BT ceramic sample and the glass-ceramic samples is that the dielectric constant of the BT ceramic sample increases continually with temperature up to 1300 °C, whereas the room-temperature dielectric constants of the glass-ceramic samples drop after annealing at higher temperature.

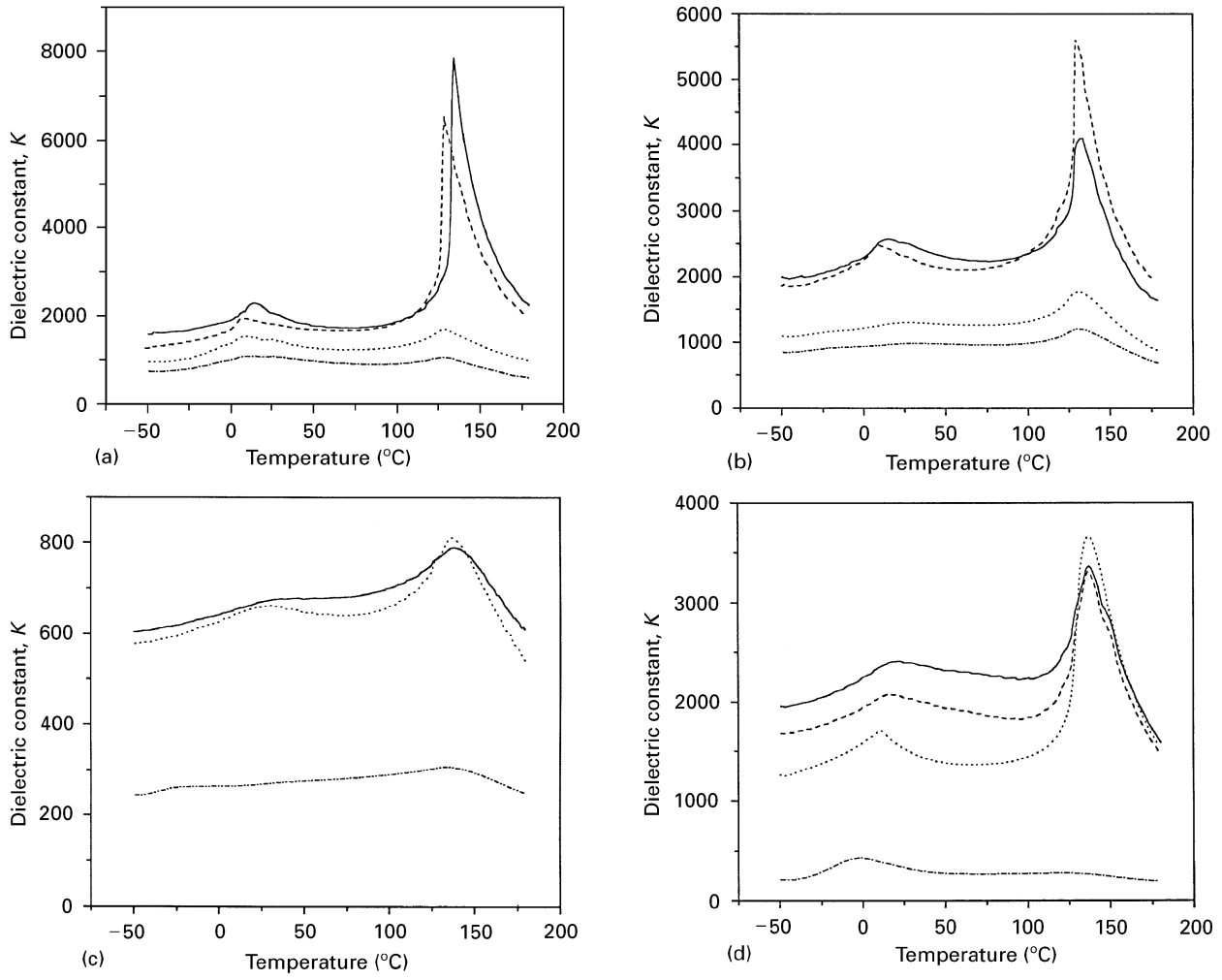

Figure 9 Temperature dependence of dielectric constant of the $BaTiO_3$ ceramic and glass-ceramic samples annealed at different temperatures in air for 1 h: (a) BT, (· — ·) 1000 °C, (· · ·) 1100 °C, (– – –) 1250 °C, (——) 1300 °C; (b) BTB, (— · · —) 850 °C, (· · ·) 900 °C, (——) 1000 °C, (– – –) 1100 °C; (c) BTBS, (— · · —) 850 °C, (——) 1000 °C, (· · ·) 1100 °C; and (d) BTAS, (— · —) 1000 °C, (——) 1200 °C, (– – –) 1250 °C, (· · ·) 1300 °C.

Although the dielectric constant of the very small $BaTiO_3$ grains is low owing to its weak ferroelectricity and increases with grain size, it is known for the polycrystalline $BaTiO_3$ that reasonably small grain sizes will enhance its room-temperature dielectric constant by virtue of the stress and/or domain-wall effects [23–26]. The grain size corresponding to the maximum room-temperature dielectric constant for $BaTiO_3$ ceramic has been reported to be about 1 μm [23], 400 nm [25], and 700 nm [26] by different groups. However, in our experiments, the room-temperature dielectric constant of the BT ceramic sample increases continually with temperature up to 1300 °C and the average grain size also increases to over 10 μm, as seen in Figs 7a and 9a, respectively. This indicates no such size effect can apparently be observed. It is believed for the BT ceramic sample that the size effect can be covered by the poor sinter when the annealing temperature is below 1300 °C, even if the intrinsic dielectric constant of $BaTiO_3$ grains is dependent on their size and decreases with the grain size beyond some critical value. On the other hand, the room-temperature dielectric constants of the glass-ceramic samples decrease with increasing annealing temperature above the sintering temperature, as shown in Fig. 9b–d. This fact indicates that such a grain-size effect on the $BaTiO_3$ dielectric constant can indeed be apparently observed in the glass-ceramic samples, because these samples can be well sintered at lower temperature and much finer grains can be achieved in the well-sintered samples. Because the grains of the BTB sample are much bigger than those of the BTAS sample, as seen in Fig. 7b and d, the decrease of the room-temperature dielectric constant for the BTB sample is not as much as that of the BTAS sample. Such a size effect in the BTBS sample is manifested not as notably as the BTAS sample by virtue of the much precipitated secondary phase in the BTBS sample. However, for all of the BT, BTB, BTBS and BTAS samples, the dielectric constants at the Curie point increase with increasing annealing temperature due to the development of the tetragonal structure and its related ferroelectricity. High room-temperature dielectric constants are obtained for the 1200 °C sintered BTAS sample and the 1000 °C sintered BTB sample with appropriate small grain sizes. The dielectric constant of the BTBS sample sintered at 1000 °C is much smaller, because a large amount of secondary phase is crystallized.

The temperature dependence curves of the dielectric constant for the BT ceramic and glass-ceramic samples also indicate that the variation in magnitude of the dielectric constant with temperature for the glass-ceramic samples is smaller than that of BT ceramic. This is attributed to the glass phase, the minor secondary

TABLE II Sintering temperatures and dielectric properties of the $BaTiO_3$ ceramic and glass-ceramic samples prepared from sol–gel derived powders

Samples	BT	BTB	BTBS	BTAS
Sintering temperature (°C)	1300	1000	1000	1200
D.c. breakdown ($kVcm^{-1}$)	25	190	280	68
Resistivity (Ω cm, 20 °C)	3×10^{10}	8×10^{11}	7×10^{12}	10^{11}
Dielectric constant, K (20 °C)	2350	2600	670	2400
Curie point (K)	7900	4090	770	3280
Dielectric loss (20 °C, 1 kHz) (%)	2.4	1.8	0.9	2.0
Max. value of $\Delta K/K_{25\,°C}$[a] (%)	29	25	9	19

[a] In the temperature range − 50 °C to 125 °C

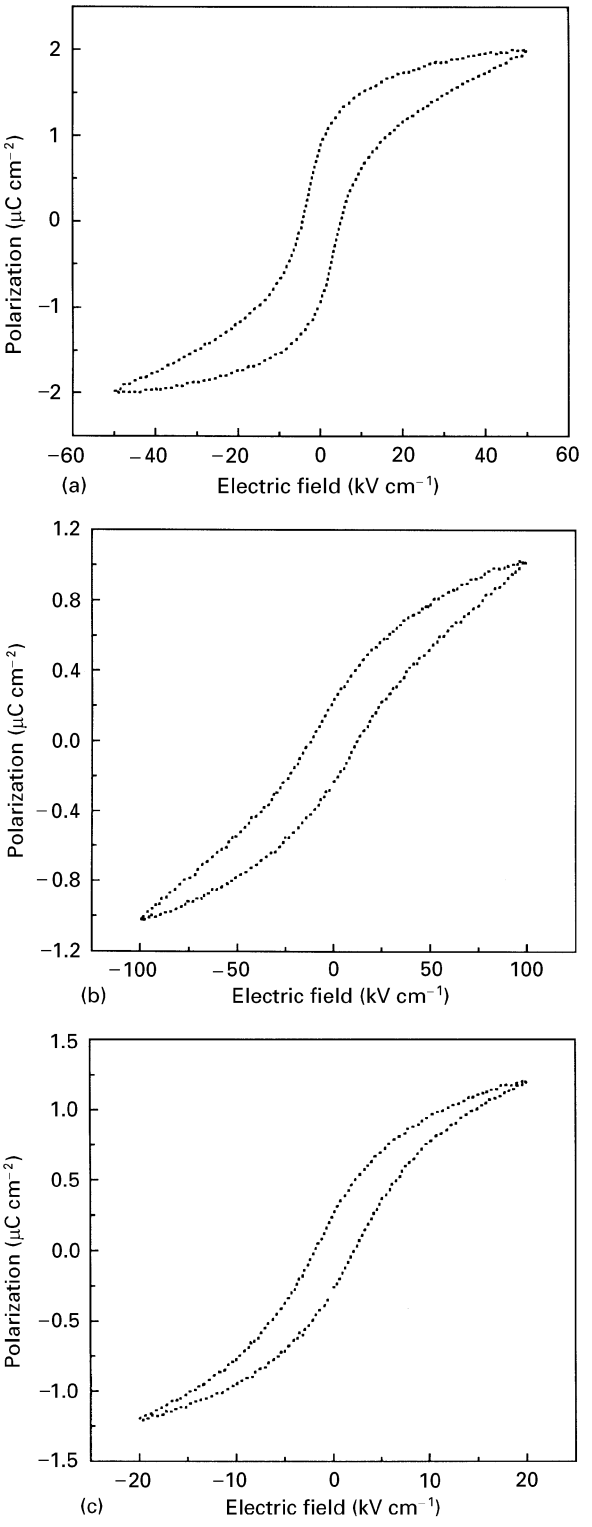

Figure 10 Ferroelectric hysteresis loops of glass-ceramic samples sintered at different temperatures in air for 1 h: (a) BTB, 1000 °C, (b) BTBS, 1000 °C and (c) BTAS, 1200 °C.

crystalline phases and the small size effect in the glass-ceramics.

The dielectric properties of the sintered BT ceramic and glass-ceramic samples are summarized in Table II. It is shown that the glass-ceramic samples have a higher resistivity, higher dielectric strength and lower dielectric loss than those of the BT ceramic sample. The good properties of the glass-ceramic samples are believed to be due to their fine-grained and well-sintered structure. These results offer great potential for these glass-ceramics in electronic component applications.

Fig. 10 shows ferroelectric hysteresis loops for BTB, BTBS and BTAS samples. These hysteresis loops show reasonable ferroelectricity of $BaTiO_3$ crystallites *in situ* grown from the gel matrix. They also show that a higher electrical field is required for the BTBS sample than for the BTB and BTAS samples. This is because a large amount of secondary $Ba_2TiSi_2O_8$ exists in the BTBS system, in other words, the volume portion of the $BaTiO_3$ phase is lower in this sample. It is seen from Fig. 10 that the remnant polarization and the saturation polarization of BTBS and BTAS samples are smaller than those of BTB sample, because the crystallites in the BTBS and BTAS sample are much smaller than those in BTB sample.

4. Conclusion

Successful preparation is reported of $BaTiO_3$-based glass-ceramics with various compositions by sintering the sol–gel derived powders together with experimental results for these samples. Compared with the pure $BaTiO_3$ ceramic sample, the glass-ceramic samples have much finer grain size and can be sintered well at lower temperature. The resistivity, dielectric strength and the dielectric loss of the glass-ceramic samples are superior to those of the ceramic sample. In spite of containing some glass phases and secondary phases, the BTB and BTAS glass-ceramic samples have high dielectric constant due to the notable size effect and the good sintering property in the glass-ceramic samples. The temperature coefficients of the dielectric constants of all glass-ceramic samples are smaller than that of BT ceramic. Good ferroelectric hysteresis loop are also observed in all these glass-ceramic samples.

Acknowledgement

This work has been partially supported by The National Advanced Materials Research Project of China.

References

1. G. H. MAHER, in "Ceramic Transactions: Ceramic Thin and Thick Films", Vol. 11, edited by B. V. Hiremath (American Ceramic Society, Westerville, OH, 1990) pp. 429–35.
2. J. J. LICARI and L. R. ENLOW, "Hybrid Microcircuit Technology Handbook: Materials, Processes, Design, Testing and Production" (Rockwell International, Anaheim, CA, 1988) pp. 114–16.
3. A. J. MOULSON and J. M. HERBERT, "Electroceramics: Materials, Properties and Application" (Chapman and Hall, London, 1990) pp. 200–3, 222.
4. L. M. LEVINSON, "Electronic Ceramic: Properties, Devices and Applications" (Marcel Dekker, New York, Basel, 1988) pp. 205–7, 339–40.
5. B. S. CHIOU, *IEEE Trans. Compon. Hybrids Manuf. Technol.* **12** (1989) 789.
6. B. S. CHIOU, K. C. LIU, J. G. DUH and M. C. CHUNG, *ibid.* **14** (1991) 645.
7. D. W. HAMER and J. V. BIGGERS, "Thick-Film Hybrid Microcircuit Technology" (Roberte Krieger, Malabar, FL, 1983) pp. 89–90.
8. F. CHAPUT, J. P. BOILOT and A. BEAUGER, *J. Am. Ceram. Soc.* **73** (1990) 942.
9. J. E. FUNK and D. R. DINGER, "Predictive Process Control of Crowded Particulate Suspensions: Applied to Ceramic Manufacturing" (Kluwer Academic, Boston, 1993) pp. 395–6.
10. A. HERCZOG, *J. Am. Ceram. Soc.* **47** (1964) 107.
11. T. KOKUBO and M. TASHIRO, *J. Non-cryst. Solids* **13** (1973) 328.
12. M. M. LAYTON and A. HERCZOG, *J. Am. Ceram. Soc.* **50** (1967) 369.
13. S. ITO, T. KOKUBO and M. TASHIRO, *J. Mater. Sci.* **13** (1978) 930.
14. D. R. ULRICH, *Solid State Technol.* **12** (1969) 30.
15. D. R. ULRICH and N. Y. LIVERPOOL, US Pat. 3649 353 (1972).
16. K. YAO, L. Y. ZHANG and X. YAO, *Chin. Sci. Bull.* **40** (1995) 694.
17. P. P. PHULE and S. H. RISBUD, *Adv. Ceram. Mater.* **3** (1988) 183.
18. A. MOSSET, I. GAUTIER-LUNEAU, J. GALY, P. STREHLOW and H. SCHMIDT, *J. Non-cryst. Solids* **100** (1988) 339.
19. J. P. GRAMMATICO, J. M. PORTO LOPEZ, *J. Mater. Sci. Mater. Electron.* **3** (1992) 82.
20. K. YAO, L. B. KONG, L. Y. ZHANG and X. YAO, J. Xi'an Jiaotong University, **30** (1996) 40–4.
21. K. YAO, PhD thesis, Xi'an Jiaotong University, Xi'an, China (1995) pp. 49–51, 94–6.
22. K. UCHINO, E. SADANAGA and T. HIROSE, *J. Am. Ceram. Soc.* **72** (1989) 1555.
23. G. ARLT, D. HENNINGS and G. DE WITH, *J. Appl. Phys.* **58** (1985) 1619.
24. A. J. BELL, A. J. MOULSON and L. E. CROSS, *Ferroelectrics* **54** (1984) 147.
25. A. S. SHAIKH, R. W. VEST and G. M. VEST, *IEEE Trans. Ultrason. Ferroelect. Frequency Control* **36** (1989) 407.
26. G. ARLT, *Ferroelectrics* **104** (1990) 217.

Received 7 May 1996
and accepted 7 January 1997